Coordination Unsaturation in the Iron Tetrathiometalate Complexes. Synthesis and Structural Characterization of the $[Fe(WS_4)_2(HCON(CH_3)_2)_2]^{2-}$ Complex Anion

P. Stremple, N. C. Baenziger, and D. Coucouvanis*

Department of Chemistry, University of Iowa Iowa City, Iowa 52242

Received December 8, 1980

Interest in the chemistry of polyheteronuclear complexes that contain iron, sulfur, and either molybdenum or tungsten derives primarily from recent studies on the Mo containing site in nitrogenase. Structural information, obtained by Mo-EXAFS[1] analyses, indicate that the proximal coordination environment around the Mo atom to ca. 3 Å consists of iron and sulfur atoms.

Recent efforts toward the synthesis and characterization of Fe–Mo–S complexes have resulted in the isolation of the "double cubanes" which contain the $Fe_6Mo_2S_{11}$ cores[2,3] and certain complexes of iron with the MS_4^{2-} ligands (M = Mo, W).[4-8] In the structurally characterized MS_4^{2-} complexes, $[(SPh)_2FeS_2MS_2]^{2-}$,[4] $[(S_5)FeS_2MS_2]^{2-}$,[5] $[(Cl_2Fe)_2MS_4]^{2-}$,[6] $[Cl_2FeMS_4]^{2-}$,[4b] $[(MoS_4)_2Fe]^{3-}$,[7] and $[(NO)_2FeS_2MS_2]^{2-}$,[8] the MS_4^{2-} "ligands" are bound as bidentate chelates to tetrahedrally coordinated iron atoms.

In this communication we report on the properties of the four-coordinate, tetrathiotungstate complex $[Fe(WS_4)_2]^{2-}$ (I)[9] and the crystal and molecular structure of the octahedral bis(dimethylformamide) "adduct" of the tetraphenyl phosphonium (PPh_4^+) salt of this anion.

The synthesis of the $(Ph_4P)_2Fe(WS_4)_2$ salt is accomplished by the reaction of $Fe(SO_4)\cdot 7H_2O$, $(NH_4)_2WS_4$, and PPh_4Cl in water.[9] We have been unable to crystallize this green solid; however, analytical and infrared spectral data are similar to those reported previously for this compound and agree with the original[9] formulation. The magnetic moment ($\mu_{eff}^{corr} = 4.72\ \mu_B$) and visible spectra [376 nm (ϵ 13 800), 428 (9600), 480 (sh), 608 (4700) in CH_2Cl_2 solution] are consistent with a tetrahedrally coordinated $Fe^{II}S_4$, $S = 2$, unit.

Cyclic voltammetry[10] of I in CH_2Cl_2 (Pt electrode) shows a one electron reduction with $E_{1/2} = -0.15$ V and $|E_{p,c} - E_{p,a}|$ slightly greater than 59 mV. The constant peak current ratio, $i_{p,c}/i_{p,a} = 1.02 \pm 0.03$, at scan rates from 20 to 500 mV/s indicate stability for the reduced $[Fe(WS_4)_2]^{3-}$ form. The chemical reduction of the bis(triphenylphosphine)iminium, $(Ph_3P)_2N^+$, salt of I proceeds readily in CH_2Cl_2 upon the addition of 1 equiv of Et_4NBH_4. A rapid color change from green to red brown is observed, and dilution with diethyl ether affords a crude precipitate of $[(Ph_3P)_2N]_2(Et_4N)Fe(WS_4)_2$. After several recrystallizations from DMF/ether mixtures, pure, red-brown crystals of the mixed cation "salt" of the $Fe(WS_4)_2^{3-}$ trianion (II) are obtained in 25% yield.[11] The X-ray powder pattern of II is virtually identical with the one obtained for the corresponding MoS_4^{2-} complex, for which a crystal structure determination has revealed the presence of the $[Fe(MoS_4)_2]^{3-}$ trianion.[7a] The magnetic moment,[12] $\mu_{eff}^{corr} = 3.77\ \mu_B$, of II, also is very similar to that obtained for the corresponding MoS_4^{2-} complex and consistent with a $S = {}^3/_2$ ground state. The cyclic voltammetry[10] of II in CH_2Cl_2 (Pt electrode) shows a reversible oxidation at $E_{1/2} = -0.15$ V and confirms the existence of the couple

$$[Fe(WS_4)_2]^{3-} \overset{-e}{\rightleftarrows} [Fe(WS_4)_2]^{2-}$$

The solution electronic spectrum of II is not sensitive to the solvents employed (CH_2Cl_2, DMF) and displays the same number of absorptions as those observed in the spectrum of the analogous $[Fe(MoS_4)_2]^{3-}$ complex.[7] However, all six of the electronic absorptions in II are hypsochromically shifted (2500–5000 cm^{-1}) relative to those in the MoS_4^{2-} analogue. The spectrum of II in DMF solution is as follows: 562 nm (ϵ 4500), 492 (10 900), 437 (15 400), 362 (13 300), 321 (22 600), 295 (25 300). The lack of solvent effects in the spectra of II is to be contrasted with the pronounced changes in the visible spectra of I in solutions of coordinating solvents. Thus, in DMF solution, the spectrum of I shows electronic absorptions at 614 nm (ϵ 1600), 428 (sh), 480 (sh), and 398 (20 100). In pyridine solution, absorptions of 580 nm (ϵ 1100), 428 (sh), 480 (sh), and 396 (16 500) are observed. The intense absorption at 396 nm in these solutions, very likely, is associated with "free" WS_4^{2-}.[13]

Addition of 1 equiv of $Fe(ClO_4)_2\cdot 6H_2O$ to a DMF solution of I causes the disappearance of the 396-nm band and results in a spectrum identical with that obtained from an equimolar mixture of $Fe(ClO_4)_2\cdot 6H_2O$ and $(NH_4)_2WS_4$ in DMF. This spectrum [540 nm, 480 (sh), 415, and 378] is similar to that of the $Cl_2FeS_2WS_2^{2-}$ complex[6] [524 nm (ϵ 530), 417 (6300), 373 (7110)] and very likely originates from a dimeric $L_xFeS_2WS_2$ complex, where L = DMF or pyridine. The solution behavior of the $Fe(WS_4)_2^{2-}$ is summarized in Scheme I.

Scheme I

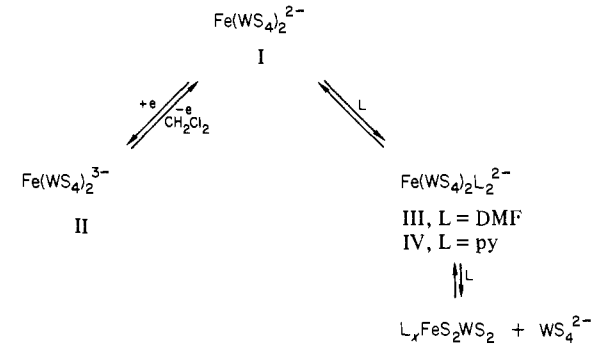

From DMF or pyridine solutions of I and following dilution with diethyl ether, red crystals of $(Ph_4P)_2[Fe(WS_4)_2(DMF)_2]$ (III) and $(Ph_4P)_2[Fe(WS_4)_2(py)_2]$ (IV) can be isolated.[14] In CH_2Cl_2

(1) (a) Cramer, S. P.; Hodgson, K. O.; Gillum, W.; Mortenson, L. E. *J. Am. Chem. Soc.* **1978**, *100*, 3398–3407. (b) Cramer, S. P.; Hodgson, K. O.; Mortenson, L. E.; Stiefel, E. I.; Chisnell, S. R.; Brill, W. S.; Shah, V. K. *Ibid.* **1978**, *100*, 3814–3819.

(2) (a) Wolff, T. E.; Berg, J. M.; Hodgson, K. O.; Frankel, R. B.; Holm, R. H. *J. Am. Chem. Soc.* **1979**, *101*, 4140–4150. (b) Wolff, T. E.; Berg, J. M.; Power, P.P.; Hodgson, K. O. Holm; R. H. *Inorg. Chem.* **1980**, *19*, 430–437. (c) Wolff, T. E.; Power, P. P.; Frankel, R. B.; Holm, R. H. *J. Am. Chem. Soc.* **1980**, *102*, 4694–4703.

(3) (a) Christou, G.; Garner, C. D.; Mabbs, F. E.; King, T. S. *J. Chem. Soc., Chem. Commun.* **1978**, 740–741. (b) Christou, G.; Garner, C. D.; Mabbs, F. E. *Inorg. Chim. Acta* **1978**, *28*, L189–L190. (c) Christou, G.; Garner, C. D.; Miller, R. M.; King, T. S. *J. Inorg. Biochem.* **1979**, *11*, 349–353.

(4) (a) Coucouvanis, D.; Simhon, E. D.; Swenson, D.; Baenziger, N. C. *J. Chem. Soc., Chem. Commun.* **1979**, 361–362. (b) Tieckelmann, R. H.; Silvis, H. C.; Kent, T. A.; Huynh, B. H.; Waszczak, J. V.; Teo, B. K.; Averill, B. A. *J. Am. Chem. Soc.* **1980**, *102*, 5550–5559.

(5) Coucouvanis, D.; Baenziger, N. C.; Simhon, E. D.; Stremple, P.; Swenson, D.; Kostikas, A.; Simopoulos, A.; Petrouleas, V.; Papaefthymiou, V. *J. Am. Chem. Soc.* **1980**, *102*, 1730–1732.

(6) Coucouvanis, D.; Baenziger, N. C.; Simhon, E. D.; Stremple, P.; Swenson, D.; Kostikas, A.; Simopoulos, A.; Petrouleas, V.; Papaefthymiou, V. *J. Am. Chem. Soc.* **1980**, *102*, 1732–1734.

(7) (a) Coucouvanis, D.; Simhon, E. D.; Baenziger, N. C. *J. Am. Chem. Soc.* **1980**, *102*, 6644–6646. (b) McDonald, J. W.; Friesen, G. D.; Newton, W. E. *Inorg. Chim. Acta* **1980**, *46*, L79–L80.

(8) Coucouvanis, D.; Simhon, E. D.; Stremple, P.; Baenziger, N. C. *Inorg. Chim. Acta* **1981**, 53, L135-L137.

(9) Müller, A.; Sarkar, S. *Angew. Chem., Int. Ed. Engl.* **1977**, *16*, 705–707.

(10) Cyclic voltammetry in CH_2Cl_2, 0.1 M in tetrabutylammonium perchlorate. A three electrode configuration was used, and the redox potentials were recorded relative to SCE. Solutions were approximately 10^{-3} M in the electroactive species.

(11) Anal. Calcd. for $[(Ph_3P)_2N]_2[(C_2H_5)_4N]Fe(WS_4)_2\cdot 2DMF$: C, 50.78; H, 4.65; N, 3.44; S, 12.61; W, 18.07. Found: C, 51.55; H, 4.73; N, 3.35; S, 12.32; W, 18.25.

(12) Determined in acetone-d_6 solution for I and in Me_2SO-d_6 solution for II by an NMR technique as described by: Evans, D. F. *J. Chem. Soc.* **1959**, 2003–2005.

(13) Diemann, E.; Müller, A. *Coord. Chem. Rev.* **1973**, *10*, 79–122.

0002-7863/81/1503-4601$01.25/0

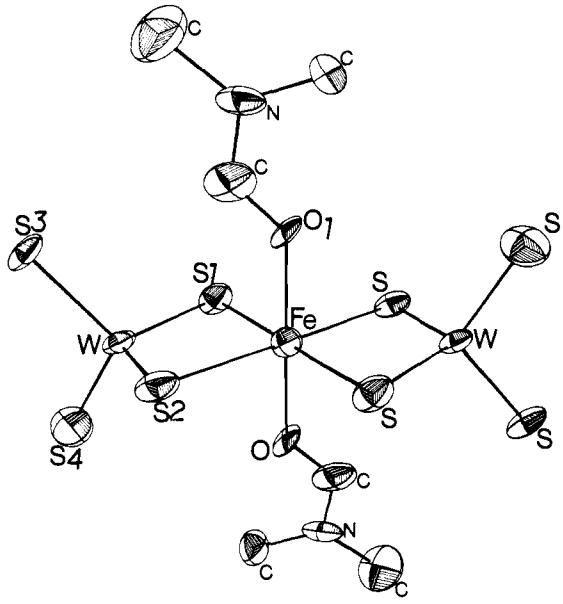

Figure 1. Structure and labeling of the $Fe(WS_4)_2(DMF)_2^{2-}$ anion. Thermal elliposoids are drawn by ORTEP (Johnson, C. K. ORNL-3794, Oak Ridge National Laboratory, Oak Ridge, TN, 1965) and represent the 50% probability surfaces.

solution the spectra of III and IV are similar to the spectrum of I, in the same solvent, and indicate a dissociation of the pyridine or DMF ligands.

Single crystals of III can be obtained by the slow diffusion of diethyl ether into a DMF solution of III. Single-crystal, X-ray diffraction data[15] were collected on a Picker-Nuclear FACS-I automated diffractometer with graphite monochromatized Mo Kα radiation (γ = 0.7107, $2\theta_m$ = 12.20°). The data were corrected for Lorentz, polarization, and absorption (μ = 48.1 cm^{-1}) effects, and the structure was solved by conventional Patterson and Fourier techniques. Refinement by full matrix, least-squares calculations has converged to a conventional R value of 0.031 by using anisotropic thermal parameters for all nonhydrogen atoms. The hydrogen atoms, at their calculated positions, were included in the structure factor calculations but were not refined.

The structure of the anion is shown in Figure 1, and structural details are presented in Table I. In the crystal, the six-coordinate iron atom in the anion is located on a crystallographic center of symmetry and is coordinated by two bidentate WS_4^{2-} ligands and two DMF molecules in a trans arrangement. The FeS_4 unit is required by symmetry to be planar. The O–Fe–O linear unit is canted 2.9° from being normal to the FeS_4 plane. At 3.044 (1) Å, the Fe–W distance is significantly longer than that found in the $[(S_5)FeS_2WS_2]^{2-}$ anion,[5] 2.753 (3) Å, and the $[Cl_2FeS_2WS_2]^{2-}$ anion,[16] 2.821 (2) Å. The iron atoms in these anions are tetrahedrally coordinated and contain a chelated WS_4^{2-} ligand. The rather long Fe^{II}–S bonds in III, 2.489 (1) and 2.534 (2) Å, also are longer than the correspondng bond lengths in $[(S_5)FeS_2WS_2]^{2-}$ 2.260 (7) and 2.280 (7) Å (Table I). The mean Fe–S bond length in III (2.511 Å) is comparable to the corresponding value for the Fe–S bond of the central Fe^{II}–S_6 unit in the $[W_2Fe_7S_8(SC_7H_7)_{12}]^{4-}$ cluster[2b] (2.566 Å). Collectively, and compared to structural parameters for the $[(S_5)FeS_2WS_2]^{2-}$ anion, the longer W–Fe distance, larger W–S–Fe angle, and shorter W–S_{bridge} bonds in III suggest a weakly coordinated WS_4^{2-} ligand in the octahedral anion. The apparent dissociation of WS_4^{2-} in solution is consistent with the crystallographic results. The Fe–O bond length of 2.082 (4) Å is only slightly shorter than the Fe–O bond in the $Fe(DMF)_6^{2+}$ counterion of the $[Fe(DMF)_6][Cl_2FeWS_4]$ complex,[16] of 2.098 (9) Å.

Table I. Selected Structural Parameters[a] in the $[Fe(WS_4)_2(DMF)_2]^{2-}$ (A), $[(S_5)FeS_2WS_2]^{2-}$ (B),[b] and WS_4^{2-} (C)[c] Anions

	A	B	C
	Bond Lengths, Å		
Fe–W	3.044 (1)	2.753 (3)	
W–S_1	2.214 (2)	2.240 (6)	
W–S_2	2.213 (1)	2.269 (7)	
W–S_3	2.169 (2)	2.142 (6)	2.165 (8)[d]
W–S_4	2.159 (2)	2.172 (8)	
Fe–S_1	2.534 (2)	2.260 (7)	
Fe–S_2	2.489 (1)	2.280 (7)	
Fe–O	2.082 (4)		
S_1–S_2	3.593 (3)	3.588 (6)	3.54 (3)[d]
S_1–S_2'	3.510 (3)		
C–O	1.232 (6)		
	Bond Angles, deg		
W–Fe–W	179.93 (1)		
Fe–S–W	80.0 (5)[d]	74.9 (6)[d]	
S_1–W–S_2	108.55 (8)		
S_1–Fe–S_2	91.35 (6)		
S_1–Fe–S_2'	88.65 (6)		
S_1'–Fe–O	91.73 (13)		
S_1–Fe–O	88.27 (13)		

[a] For all structures the reported structural parameters are in analogous reference to the labeling shown in Figure 2. [b] From ref 5. [c] From ref 17. [d] Mean value of the chemically equivalent bonds or angles, $\sigma = [\sum_{i=1}^{N}(x_i - x)^2/N - 1]^{1/2}$.

It is apparent that the MS_4^{2-} anions are unique in their ability to delocalize charge in the MS_4^{2-}–M′ complexes by accepting electron density, in low lying, unoccupied M-d orbitals. Not only is there a delocalization of charge in these complexes, but very often they undergo reversible reductions by one or even two electrons. Such reductions have been reported for the $[M'(MS_4)_2]^{2-}$ complexes (M′ = Ni, Pd, Pt; M = Mo or W)[18] and for $[Co(WS_4)_2]^{2-}$.[19] In the MS_4–Fe complexes reversible one electron reductions are observed for the $[(FeCl_2)_2MoS_4]^{2-}$[20] and $[Fe(WS_4)_2]^{2-}$ complexes, and the stable $[Fe(MS_4)_2]^{3-}$ trianion has been isolated[7] and structurally characterized.[7a]

The significance of the low potential reductions, observed with certain M′–MS_4 complexes, becomes apparent when these complexes are considered as possible catalysts for the reductions of substrate molecules. In such M′–MS_4 complexes, the MS_4^{2-} ligands could serve as convenient electron storage and relay sites. The propensity of the $[Fe(MS_4)_2]^{2-}$ complexes to accept electrons is further illustrated in the pronounced tendency of the $[Fe(WS_4)_2]^{2-}$ complex toward the formation of adducts with σ electron donor molecules. The isolation of the bis(dimethylformamide) and dipyridine adducts of the $[Fe(WS_4)_2]^{2-}$ complex shows for the first time that the $[Fe(MS_4)_2]^{2-}$ complexes can function as coordinatively unsaturated species.

The difficulty in the isolation of the $[Fe(MoS_4)_2]^{2-}$ dianion may be associated with the tendency of the $[Fe(MS_4)_2]^{2-}$ anions to interact with Lewis bases or polymerize in the absence of bases.[21]

The demonstration that the MS_4^{2-} anions can serve as chelating ligands in pseudo octahedral complexes adds a new dimension to the considerations of the MoS_4 unit as possible structural component of the nitrogenase active site.

(14) Anal. Calcd for $(PPh_4)_2Fe(WS_4)_2(DMF)_2$ (III): C, 43.09; H, 3.61; N, 1.86; S, 17.04; Fe, 3.71; W, 24.43. Found: C, 43.74; H, 3.67; N, 2.04; S, 17.13; Fe, 3.56; W, 25.10. Anal. Calcd for $(PPh_4)_2Fe(WS_4)_2(py)_2$ (IV): C, 45.91; H, 3.32; N, 1.84; Fe, 3.68. Found: C, 45.93; H, 3.59; N, 2.34; Fe, 3.63.

(15) Crystal and refinement data for $(Ph_4P)_2Fe(WS_4)_2(DMF)_2$: cell dimensions a = 10.101 (1), b = 18.612 (2), c = 15.851 (2) Å; β = 103.25 (1)°; space group $P2_1/n$; Z = 2; d_{calcd} = 1.74, d_{obsd} = 1.73 g/cm^3; reflections used, $F^2 > 3\sigma(F^2)$, 4316, unique reflections, 5101; parameters 325; $2\theta_{max}$ = 50°.

(16) Coucouvanis, D.; Stremple; P.; Baenziger, N. C., unpublished results.

(17) Sasvari, K. *Acta Crystallogr.* **1963**, *16*, 719.

(18) (a) Callahan, K. P.; Piliero, P. A. *J. Chem. Soc., Chem. Commun.* **1979**, 13–14. (b) Callahan, K. P.; Piliero, P. A. *Inorg. Chem.* **1980**, *19*, 2619–2626.

(19) Muller, A.; Jostes, R.; Flemming, V.; Potthast, R. *Inorg. Chim. Acta* **1980**, *44*, L33–L35.

(20) Unpublished observations; work in progress.

(21) Work in progress includes a careful examination of the chemistry of the $[Fe(MoS_4)_2]^{n-}$ system.

Acknowledgment. This work has been generously supported by grants from the National Science Foundation (CHE-79-0389), the National Institutes of Health (GM 26671-01), and a NATO Research Grant (No. 1321). The computing expenses have been covered by grants from the University of Iowa, Graduate College.

Supplementary Material Available: Structure factors and positional coordinates for $(Ph_4P)_2[Fe(WS_4)_2(HCON(CH_3)_2)_2]$ (22 pages). Ordering information is given on any current masthead page.

Editing of ^{13}C NMR Spectra. A Pulse Sequence for the Generation of Subspectra

M. R. Bendall,* D. M. Doddrell, and D. T. Pegg

School of Science, Griffith University
Nathan, Queensland, 4111, Australia
Received March 9, 1981

In this article we describe a simple multinuclear pulse sequence, sequence 1, which enables the acquisition of ^{13}C spectra containing just CH_3 and CH resonances or just CH_2 and quaternary carbon resonances. The sequence has the advantage of accurate cancellation of the unwanted resonances.

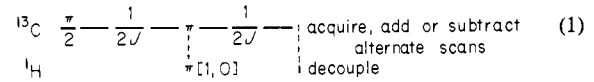

(1)

The key to the mechanism of this sequence, illustrated in Figure 1, is the judicious use of the π[H;1,0] refocusing pulse, [1,0], signifying that the pulse is applied for alternate scans only. Figure 1d,i illustrates the outcome of the sequence for a CH and CH_2 group, respectively, at the point at which the decoupling field is introduced, for scans in which the π[H] pulse is omitted, and Figure 1e,j illustrates the outcome for scans in which a π[H] pulse is used. For a CH_3 group (not illustrated[it can be easily shown that the various carbon vectors are refocused along the y or $-y$ axis as for a CH group in Figure 1d,e. Assuming proton coupling is small, quaternary carbons are unaffected by the sequence except that precession due to chemical shift and field inhomogeneity is refocused back to the y axis as for a CH_2 group in Figure 1i,j. From Figure 1d,e,i,j it is clear that alternate use of the π[H] pulse and addition of alternate scans produces a spectrum containing only CH_2 and quaternary carbon resonances, and subtraction of alternate scans produces a spectrum containing only CH and CH_3 carbon resonances. Spectra of cholesterol, obtained in this manner, are shown in Figure 2. As often occurs in ^{13}C spectra, several of the cholesterol CH and CH_2 resonances are close together. Cancellation of signals, rather than inversion of some signals relative to others, is obviously preferable in such instances and is necessary for quantitative studies.

Spectral editing of this sort has been recently achieved by using the INEPT sequence.[1,2] However, sequence 1 has clear advantages over the INEPT sequence. Single-bond CH coupling constants vary somewhat; so an average J value must be used in setting the free precession periods in sequence 1 and the INEPT sequence. Divergence from this average J value leads to residual carbon signals instead of exact cancellation, but in general the cancellation is more exact for sequence 1 than for INEPT. For example, by using the INEPT sequence CH_2 and CH_3 signals may be cancelled after a total free precession period for the carbon vectors of $(2J)^{-1}$ s.[1] Although the INEPT sequence is marginally less sensitive to error in J for the cancellation of CH_3 signals than is sequence 1, it is straightforward to show that a 5 error in J leads to a 15.6% residual CH_2 signal for INEPT, whereas for sequence

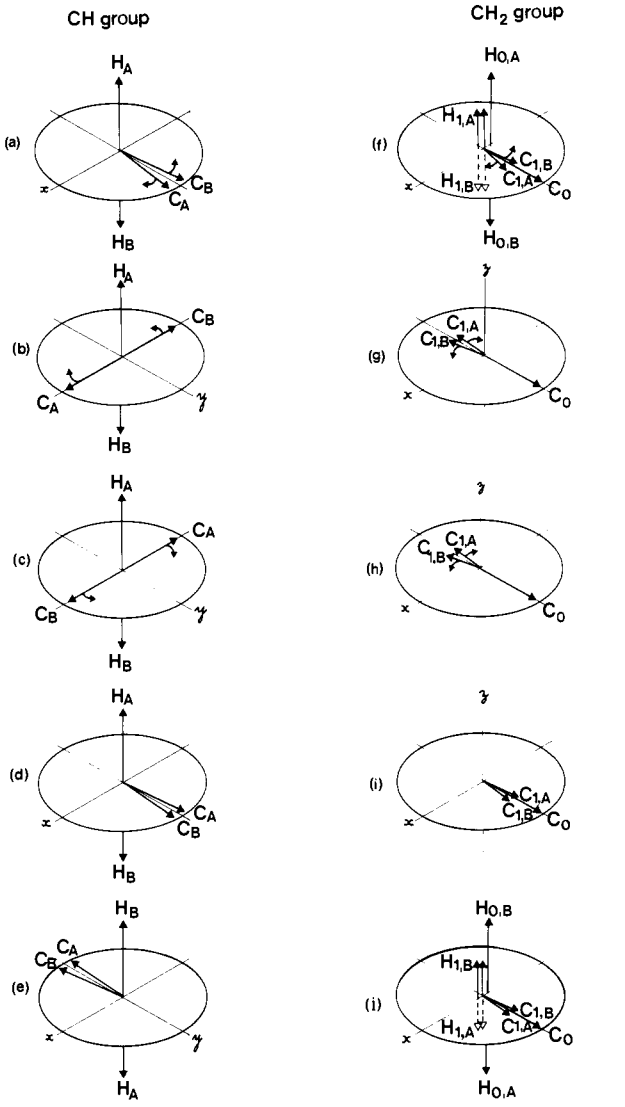

Figure 1. Because precession in the rotating frame due to chemical shift and field inhomogeneity is refocused at the end of the free precession period by the π[C] pulse, precession due only to proton coupling is shown. (a) After a $(\pi/2)$[c,x] pulse, the magnetization vector of ^{13}C nuclei coupled to protons, which is initially along the y axis of the rotating frame, splits into a clockwise rotating vector (C_A) and an anticlockwise rotating vector (C_B), corresponding to whether the protons are in the $+z$ (H_A) or $-z$ eigenstate (H_B), respectively. (b) After the first period of $(2J)^{-1}$ s, where J is the single-bond coupling constant, C_A and C_B have precessed 90°. (c) A π[C] pulse along the y axis, say, swaps C_A and C_B. (d) After the second period of $(2J)^{-1}$ s, C_A and C_B are refocused along the y axis. (e) If after the first period of $(2J)^{-1}$ s, a π[H] pulse is introduced, the precessional direction of the C_A and C_B vectors are reversed and refocused along the $-y$ axis after the second period of $(2J)^{-1}$ s. (f)–(j) Vector positions for a CH_2 group at the same stages during the sequence as shown for a CH group in (a)–(e), respectively. The carbon magnetization vector splits into three vectors $C_{1,A}$, $C_{1,B}$, and C_0 corresponding to whether the attached protons are both in the $+z$ eigenstate ($H_{1,A}$), both in the $-z$ eigenstate ($H_{1,B}$), or are opposed ($H_{0,A}$ and $H_{0,B}$).

1 the residual signal would be only 1.2% of the total. Another advantage is that, unlike INEPT, the CH/CH_3 and CH_2/quaternary subspectra can be compared directly with a normal spectrum obtained with sequence 1 but without using the π[H] pulse. In fact, if the alternate scans are averaged into two different memory blocks, the three spectra, as in Figure 2, are available from the one experiment. Again, unlike INEPT, the same spectral simplifications are obtained by using off-resonance decoupling during acquisition, and the subspectra may be obtained with or without nuclear Overhauser enhancements. Although the INEPT sequence provides a one-third theoretical advantage in sensitivity over spectra obtained with the full nuclear Overhauser en-

(1) Doddrell, D. M.; Pegg, D. T. *J. Am. Chem. Soc.* **1980**, *102*, 6388–6390. Morris, G. A.; Freeman, R. *Ibid.* **1979**, 101, 760–761. Burum, D. T.; Ernst, R. R. *J. Magn. Reson.* **1980**, *39*, 163–168.
(2) Thomas, D. M.; Bendall, M. R.; Pegg, D. T.; Doddrell, D. M.; Field, J. *J. Magn. Reson.* **1981**, *42*, 298–306.

0002-7863/81/1503-4603$01.25/0